



ORIGINAL ARTICLE

Six novel complexes based on 5-Acetoxy-1-(6-chloro-pyridin-2-yl)-1H-pyrazole-3-carboxylic acid methyl ester derivatives: Syntheses, crystal structures, and anti-cancer activity



Yanhui Qiao^a, Yating Chen^b, Shuhua Zhang^{a,b,*}, Qiuping Huang^{b,c}, Yujie Zhang^b, Guangzhao Li^{a,*}

^a College of Chemistry, Guangdong University of Petrochemical Technology, Maoming, Guangdong 525000, China

^b Guangxi Key Laboratory of Electrochemical and Magnetochemical Functional Materials (College of Chemistry and Bioengineering), Guilin University of Technology, Guilin 541004, China

^c College of Chemistry and Engineering, Guangxi Normal University for Nationalities, Chongzuo 532200, China

Received 9 March 2021; accepted 25 May 2021

Available online 29 May 2021

KEYWORDS

Synthesis;
Crystal structure;
Copper(II) Compound;
Anti-cancer activity;
Water solubility

Abstract A novel 5-Acetoxy-1-(6-chloropyridin-2-yl)-1H-pyrazole-3-carboxylic acid methyl ester derivatives Htcdodtta (**1**), and its five complexes, $[\text{Cu}_2(\text{L}^1)_2] \cdot (\text{CH}_3\text{CN})$ (**2**), $[\text{Cu}_2(\text{L}^2)_{1.63}(\text{L}^3)_{0.37}] \cdot (\text{CH}_3\text{OH})_{0.5}$ (**3**), $[\text{Cu}_2(\text{L}^3)(\text{L}^4)] \cdot (\text{C}_2\text{H}_5\text{OH})_{0.5} \cdot (\text{CH}_3\text{OH})_{0.5}$ (**4**), $[\text{Cu}_2(\text{L}^4)(\text{L}^5)] \cdot (\text{H}_2\text{O})$ (**5**) and $[\text{Cu}_2(\text{L}^1)_{1.18}(\text{L}^2)_{0.82}]$ (**6**) have been synthesized. The Htcdodtta, HL¹-HL⁵ were formed *in-situ* reaction. HL¹-HL⁵ are homologues which possess two chiral carbons. Compounds **1–6** were characterized using single-crystal X-ray diffraction, IR, and elemental analysis. Compounds **2–6** are dinuclear copper complexes. The *in vitro* cytotoxicities of compounds **1–4** against a variety of cell lines were evaluated by MTT assays. Hela cancer cell apoptosis assay of **1** and **2** were examined by flow cytometry. The cell apoptosis in NP69, A549, Capan-2, Hela, HepG2, and HUVECs cell lines induced by compound **2** was further affirmed by cellular morphology observations.

© 2021 The Author(s). Published by Elsevier B.V. on behalf of King Saud University. This is an open access article under the CC BY-NC-ND license (<http://creativecommons.org/licenses/by-nc-nd/4.0/>).

* Corresponding authors at: College of Chemistry, Guangdong University of Petrochemical Technology, Maoming, Guangdong 525000, China (S. Zhang).

E-mail addresses: 2002010@glut.edu.cn (S. Zhang), gqli666@gdupt.edu.cn (G. Li).

Peer review under responsibility of King Saud University.



1. Introduction

With changes to living habits and the environment, cancers have become the major cause of death in both developed and developing countries. Consequently, the design and synthesis of novel anticancer agents is a key challenge for medicinal chemists (Cao et al., 2020; Pan et al., 2020; Zhang et al., 2020). In recent decades, the synthesis of pyrazole derivatives has attracted significant research attentions (Wang et al.,

Table 1 The formula and name of Htcdodtta and HL¹-HL⁵.

Comps.	formula	name
1	C ₃₀ H ₂₂ Cl ₃ N ₉ O ₁₀	1,1',1''-tris-(6-chloropyridin-2-yl)-5,5''-dihydroxy-5'-oxo-1',5'-dihydro-1H,1''H-[4,4';4',4''] terpyrazole-3,3',3''-tricarboxylic acid trimethyl ester
HL ¹	C ₃₁ H ₂₂ Cl ₃ N ₉ O ₁₀	1,8-Bis-(6-chloropyridin-2-yl)-4-[2-(6-chloropyridin-2-yl)-5-methoxycarbonyl-3-oxo-2,3-dihydro-1H-pyrazol-4-yl]-9-oxo-1,2,7,8-tetraaza-spiro[4.4]nona-2,6-diene-3,4,6-tricarboxylic acid trimethyl ester
HL ²	C ₃₃ H ₂₆ Cl ₃ N ₉ O ₁₀	1,8-Bis-(6-chloropyridin-2-yl)-4-[2-(6-chloropyridin-2-yl)-5-methoxycarbonyl-3-oxo-2,3-dihydro-1H-pyrazol-4-yl]-9-oxo-1,2,7,8-tetraaza-spiro[4.4]nona-2,6-diene-3,4,6-tricarboxylic acid 4,6-diethyl ester 3-methyl ester
HL ³	C ₃₂ H ₂₄ Cl ₃ N ₉ O ₁₀	1,8-Bis-(6-chloropyridin-2-yl)-4-[2-(6-chloropyridin-2-yl)-5-methoxycarbonyl-3-oxo-2,3-dihydro-1H-pyrazol-4-yl]-9-oxo-1,2,7,8-tetraaza-spiro[4.4]nona-2,6-diene-3,4,6-tricarboxylic acid 4-ethyl ester 3,6-dimethyl ester
HL ⁴	C ₃₃ H ₂₆ Cl ₃ N ₉ O ₁₀	1,8-Bis-(6-chloropyridin-2-yl)-4-[2-(6-chloropyridin-2-yl)-5-methoxycarbonyl-3-oxo-2,3-dihydro-1H-pyrazol-4-yl]-9-oxo-1,2,7,8-tetraaza-spiro[4.4]nona-2,6-diene-3,4,6-tricarboxylic acid 3,6-dimethyl ester 4-propyl ester
HL ⁵	C ₃₄ H ₂₈ Cl ₃ N ₉ O ₁₀	1,8-Bis-(6-chloropyridin-2-yl)-4-[2-(6-chloropyridin-2-yl)-5-methoxycarbonyl-3-oxo-2,3-dihydro-1H-pyrazol-4-yl]-9-oxo-1,2,7,8-tetraaza-spiro[4.4]nona-2,6-diene-3,4,6-tricarboxylic acid 4-butyl ester 3,6-dimethyl ester

2018; Fustero et al., 2011) because of their potential applications in medicinal chemistry such as analgesic (Gürsoy et al., 2000), therapeutic (Jiang et al., 1990; Mohareb et al., 2012; Anzai et al., 2004), antipyretic (Palkar et al., 1969), antidepressant (Bailey et al., 1985); and anti-inflammatory agents (Badawey and El-Ashmawey, 1998). For example, 3-phenylimidazo (Pan et al., 2020; Cao et al., 2020; Pan et al., 2020; Zhang et al., 2020; Wang et al., 2018; Fustero et al., 2011; Gürsoy et al., 2000; Jiang et al., 1990; Mohareb et al., 2012; Anzai et al., 2004; Palkar et al., 1969; Bailey et al., 1985; Badawey and El-Ashmawey, 1998; Ali et al., 2014; Das et al., 2008; Huang et al., 1813; Qin et al., 2013; Kalinowska-Lis et al., 2014; Ng et al., 2013; Ambika et al., 2013; Pelosi et al., 2010; Katsarou et al., 2008; Liu and Gust, 2013; Qin et al., 2017; Zhao et al., 2014; González-Álvarez et al., 2013; Zhang et al., 2016; Qin et al., 2020; Psomas and Kessissoglou, 2013; Brown et al., 1980; Fernández-Bachiller et al., 2010; Darrenm et al., 2010; Sánchez-Delgado et al., 1998; Tardito et al., 2011; Budzisz et al., 2009; Miernicka

et al., 2008; Yang et al., 2019; Allen et al., 1991; Ciolkowski et al., 2009; Carey et al., 2007; Xiao et al., 2015; Xiao et al., 2015; Brown and Altermatt, 1985; Brese and O'keeffe, 1991; Brown, 2009; Neese, 2012; Kossmann and Neese, 2010; Qin et al., 2018; Qin et al., 2018; Qin et al., 2015; Zhang et al., 2019; Liang et al., 1994; Baryshnikov et al., 2013; Gusev et al., 2017; Alley et al., 1988; Chen et al., 2013; Sheldrick, 2015; Dolomanov et al., 2009) thiazol-6-one has been reported to show potency towards *Renal UO-31* and *CNS SNB-75* cancer cell lines (Ali et al., 2014). In addition, the biological activities of pyrazole derivatives have been found to be affected by electronegative of free radical substituents (Das et al., 2008). Recently, our group has reported the novel pyrazole derivative of methyl 5-(acetyloxy)-1-(6-bromo-2-pyridinyl)-1H-pyrazole-3-carboxylate (Huang et al., 2017).

Similarly, copper coordination complexes have attracted significant research attention owing to their various biological activities, including their antibacterial (Qin et al., 2013; Kalinowska-Lis et al., 2014; Ng et al., 2013; Ambika et al., 2013), antiviral (Pelosi et al., 2010), antileukemic (Katsarou et al., 2008), anticancer (Liu and Gust, 2013; Qin et al., 2017; Zhao et al., 2014; González-Álvarez et al., 2013; Zhang et al., 2016; Qin et al., 2020), anti-inflammatory (Psomas and Kessissoglou, 2013; Brown et al., 1980), and anti-neurodegenerative properties (Fernández-Bachiller et al., 2010). In recent years, copper complexes have been considered good substitutes for platinum-based complexes as potential antitumor drugs (Darrenm et al., 2010). It was reported that copper ion chelations resulting in suppressed angiogenesis and decreased tumour volume have been demonstrated by some animal studies. Qin et al. (2017, 2020) copper ions also can change the metabolism of cancer cells, causing differentiation of the reactions of tumour cells and normal cells. Accordingly, several copper(II) complexes with antitumor properties have been described in recent decades (Liu and Gust, 2013; Qin et al., 2017; Zhao et al., 2014; González-Álvarez et al., 2013; Zhang et al., 2016; Qin et al., 2020). In additional, the compounds based on both copper and pyridine and its derivatives have received much attention. For example, Sánchez-Delgado et al. reported a number of new M-CTZ complexes (M = Ru, Rh, Cu, Pt, and Au, CTZ is clotrimazole) (Sánchez-Delgado et al., 1998). Tardito et al. Reported a number of Pyrazole – pyridine ligands and the corresponding Cu(II) complexes (Tardito et al., 2011). The thioether-free pyrazole-pyridine ligands 5-(2-hydroxy-ybenzoyl)-3-methyl-1-(2-pyridinyl)-1H-pyrazole-4-phosphonic acid dimethyl ester (L^{44a}) and 5-(2-hydroxyphenyl)-3-methyl-1-(2-pyridinyl)-1H-pyrazole-4-carboxylic acid methyl ester (L^{44b}) and the corresponding Cu(II) complexes [Cu(L^{44a})Cl₂], [Cu(L^{44b})Cl₂], [Cu(L^{44a})₂](ClO₄)₂, and [Cu(L^{44b})₂](ClO₄)₂ have been synthesized and evaluated as potential anticancer compounds (Budzisz et al., 2009; Miernicka et al., 2008). Yang Ping et al. reported three copper compounds [Cu(L^{A-C})₂].nDMF (L^A is 3-hydroxy-N-[1-(pyrazin-2-yl)ethylidene]benzene-1-carbohydrazonato, L^B is 2-hydroxy-N-[1-(pyrazin-2-yl)ethylidene]benzene-1-carbohydrazonato, and L^C is 4-hydroxy-N-[1-(pyrazin-2-yl)ethylidene]benzene-1-carbohydrazonato) (Yang et al., 2019).

In the present study, we have attempted to combine the advantages of copper compounds and pyrazole derivatives to prepare anticancer compounds. Accordingly, we have synthesized the five novel copper coordination complexes [Cu₂(L¹)₂].(CH₃CN) (2), [Cu₂(L²)_{1.63}(L³)_{0.37}].(CH₃OH)_{0.5} (3), [Cu₂(L³)

(L⁴)]·(C₂H₅OH)_{0.5}·(CH₃OH)_{0.5} (**4**), [Cu₂(L⁴)(L⁵)]·(H₂O) (**5**), [Cu₂(L¹)_{1.18}(L²)_{0.82}] (**6**) and one novel organic compound Htc-dodtta (**1**) using 5-acetoxy-1-(6-chloro-pyridin-2-yl)-1H-pyrazole-3-carboxylic acid methyl ester (**a**) as reactant. Herein, the *in-vitro* cytotoxicities of **1–4** against six cancer and normal cell lines were evaluated by MTT assay. Herein, the formula and name of compounds Htc-dodtta and HL¹-HL⁵ were listed in the Table 1.

2. Results and discussion

2.1. Synthesis

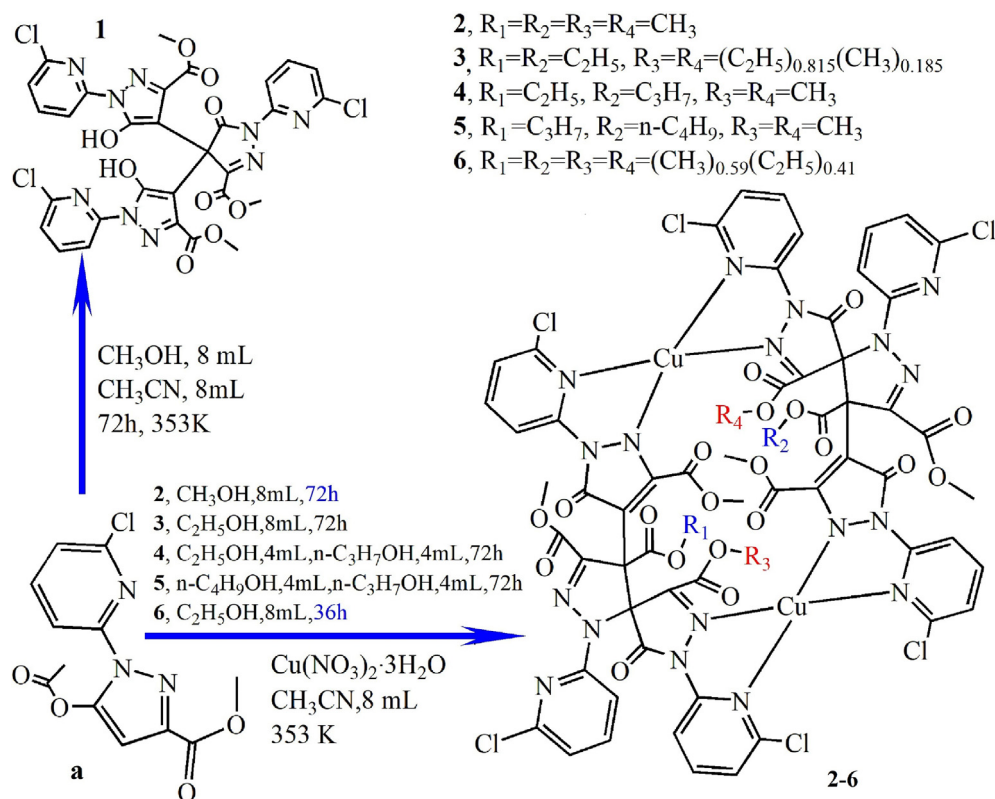
The reaction between compound **a** and Cu(NO₃)₂·3H₂O was conducted by the solvothermal method in methanol/acetonitrile (1:1) in order to synthesize new pyridyl-pyrazol-3-one derivatives (Scheme 1). As a result, the dinuclear copper complexes [Cu₂(L¹)₂](CH₃CN)₂ (**2**) was obtained. Herein, HL¹, which has two chiral centres, was synthesized *in-situ* reaction. Maybe copper ions play a catalytic role in the pyridyl-pyrazol-3-one derivatives synthesis system.

To study the role of the copper ions in the reaction, Ni²⁺ and Co²⁺ ions were used to replace Cu²⁺ ions in the reaction. However, these substitutions led only to the production of unknown white precipitates which have not been characterized because the white precipitates were mixture and were impossible characterized.

Using the same *in-situ* synthesis conditions but without copper ion, compound **1** was produced in high purity

(Scheme 1). The possible formation mechanism of compound **1** is shown in Scheme S1. Furthermore, compound **2** was produced in progressively lower yields when the molar ratio of Cu(NO₃)₂·3H₂O to **a** was decreased stepwise from 1:1 to 1:9. Compound **1** was also formed when the molar ratio was decreased to 1:10. The results indicated that copper ions play a critical role in the formation of HL¹. It must be noted that the divalent copper was reduced to the monovalent copper during the reaction.

Using the same *in-situ* synthesis conditions but the mixed solution methanol/acetonitrile (1:1) was replaced by the mixed solution ethanol/acetonitrile (1:1), compound **3** was produced in high purity (Scheme 1). Herein, we found that there exists transesterification between HL¹ and ethanol and formed two new ligands HL² and HL³. Furthermore, 3,4,6-tricarboxylic acid trimethyl ester of HL¹ changed 3,4,6-tricarboxylic acid 4,6-diethyl ester 3-methyl ester of HL² and 3,4,6-tricarboxylic acid 4-ethyl ester 3,6-dimethyl ester of HL³. we decreased reaction time, complex **6** was prepared while the degree of ester group exchange was significantly reduced. This result indicates that the lipid exchange reaction is related to the reaction time. In order to understand transesterification, we used ethanol and n-propanol mixed dissolution (1:1) and n-propanol and n-butanol (1:1) mixed solvents instead of the methanol in the mixed solvent of methanol and acetonitrile (1:1). Complexes **4** and **5** were prepared, respectively. The results indicated that the transesterification rate is basically the same for ethanol, n-propanol and n-butanol. And transesterification occurs mainly in the 4th position of the HL¹ ligand.



Scheme 1 Synthesis routes for 1-6.

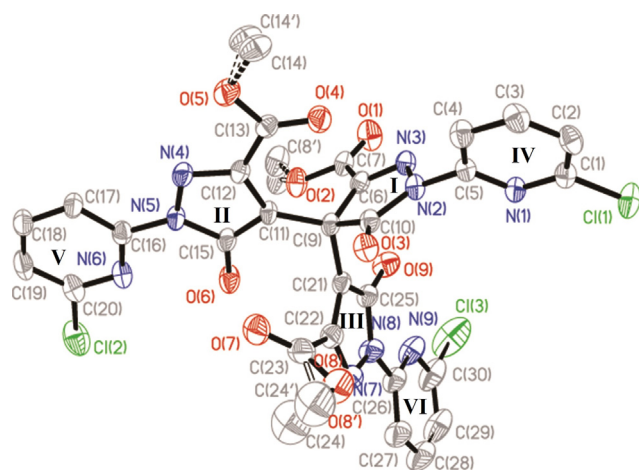


Fig. 1 Molecular structure of **1**. Displacement ellipsoids are drawn at 30% probability level. Part H atoms are omitted for clarity.

2.2. Crystal structures

2.2.1. Crystal structure of **1**

The structure of **1** is shown in Fig. 1. Single-crystal X-ray diffraction analysis revealed that **1** crystallises in the triclinic with space group $P\bar{1}$. All bond lengths in the pyrazole rings (**II** and **III**) show partial double-bond character, which indicates the delocalization of the π -electronic system throughout the pyrazole rings (Huang et al., 1813). The bond angles and bond lengths are within the normal ranges for a pyrazole ring (Table S1), and are similar to those reported for 5-(acetyloxy)-1-(6-bromo-2-pyridinyl)-1H-pyrazole-3-carboxylate (Huang et al., 1813) and the literature values (Allen et al., 1991). The C25-O9 and C15-O6 bond lengths are 1.336(5) and 1.330(4) Å, respectively. The values of the bond lengths are similar to that reported for a pyrazole-OH bond (1.329 Å) (Huang et al., 1813; Ciolkowski et al., 2009). However, C9 is sp^3 hybridised in ring **I**. The C9-C11, C9-C10, C9-C21, and C9-C6 bond lengths are 1.510(4), 1.533(5), 1.528(5), and 1.518(5) Å, respectively, which are consistent with a single bond of a sp^3 - sp^2 hybrid orbital (the average length of a C-C sp^3 - sp^2 single bond is 1.51 Å (Allen et al., 1991)). The C10-O3 bond length is 1.195 (4) Å, which clearly indicates a carbonyl group (the average length of a C = O double bond is 1.20 Å (Carey et al., 2007), while the C6-N3 bond length is 1.269(5) Å, which clearly indicates a C = N double bond (Xiao et al., 2015; Xiao et al., 2015)). Thus, there are no protons on the N3 and O3 atoms. Of course, an electron density on the fourier maps were not found around the N3 and O3 atoms. The rings position in the same plane of pyridyl-pyrazole (**II** and **V** rings) with the substituents (O6 and ester carbonyl group) at **II** and C12 at **V** ring, which is the same as the reported compound 5-(acetyloxy)-1-(6-bromo-2-pyridinyl)-1H-pyrazole-3-carboxylate (Huang et al., 1813). The maximum deviation of the least-squares plane ($10.586x + 2.666y + 8.981z = 14.1672$) is from + 0.0968 Å (C14) to - 0.1068 Å (O4). It should be noted that ring **I** bearing the substituents (C7, C8, O1, O2 of the ester carbonyl group and O3) is co-planar ($-1.240x - 3.991y + 13.769z = 5.450$). The dihedral angle between rings **I** and **IV** is 67.4°. Compound **1** forms a dimer through weak intermolecular Cl...Cl interactions (Cl2...Cl3a, 3.673 Å,

Cl3...Cl2a, 3.673 Å, symmetry code: (a) - $x, 2 - y, 2 - z$, Fig. S1), which form a two-dimensional network through Cl...O interactions (Cl1...O7b, 3.569 Å, symmetry code: (b) $\times, y - 1, z$; Fig. S2). It must be noted that the three methyl of the ester base groups in **1** is disordered over two sets of sites in a 0.36:0.64 ratio.

2.2.2. Crystal structures of **2-6**

Complexes **2-6** (Figs. 2-6) are also dinuclear copper complexes with the different crystal system and the different space group (**2,4,5** belong to triclinic crystal system with $P\bar{1}$ space group but **3** and **6** do monoclinic crystal system with $P2_1/c$ space group) and the different ester group substituents of the HL ligands. Therefore only complex **2** is analyzed here.

Single-crystal X-ray diffraction analysis revealed that complex **2** belongs to the triclinic with space group $P\bar{1}$ (Fig. 2). The dinuclear complex **2** is constructed by two (L^1) ligands, two

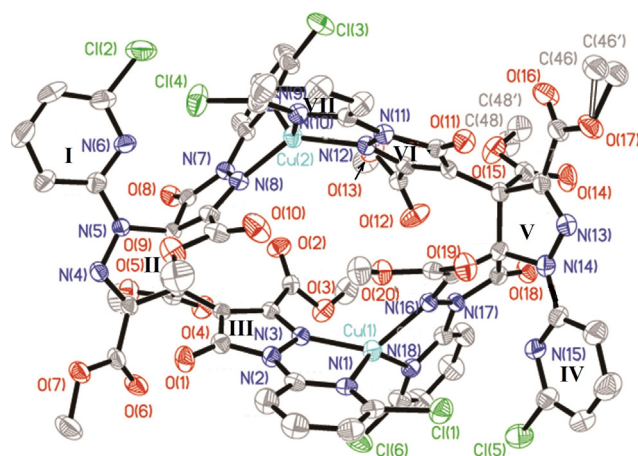


Fig. 2 Molecular structure of **2** (omitted acetonitrile molecules). Displacement ellipsoids are drawn at 30% probability level. All H atoms are omitted for clarity.

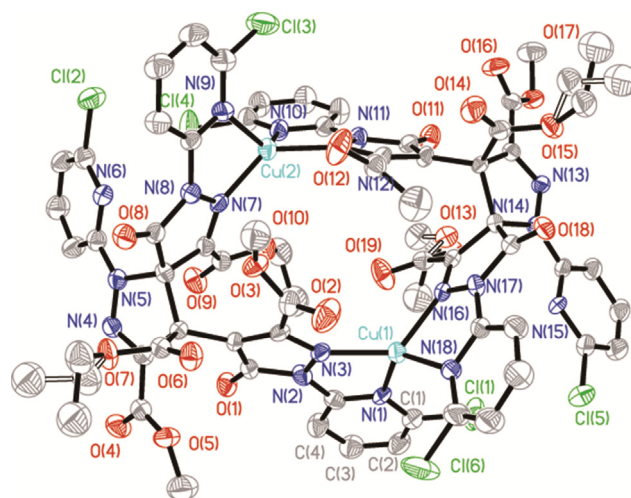


Fig. 3 Molecular structure of **3**. Displacement ellipsoids are drawn at 30% probability level. H atoms and solvent molecules are omitted for clarity.

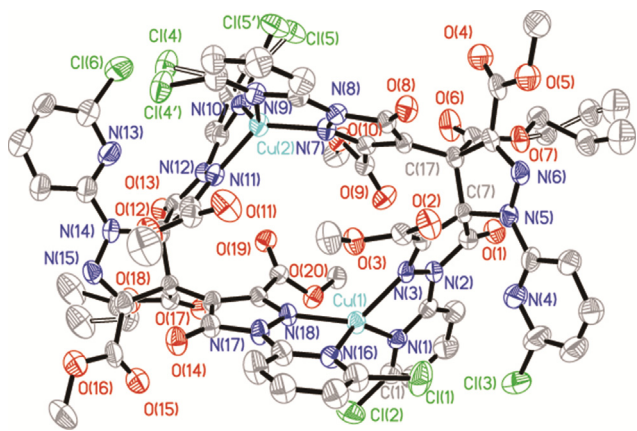


Fig. 4 Molecular structure of **4**. Displacement ellipsoids are drawn at 30% probability level. H atoms and solvent molecules are omitted for clarity.

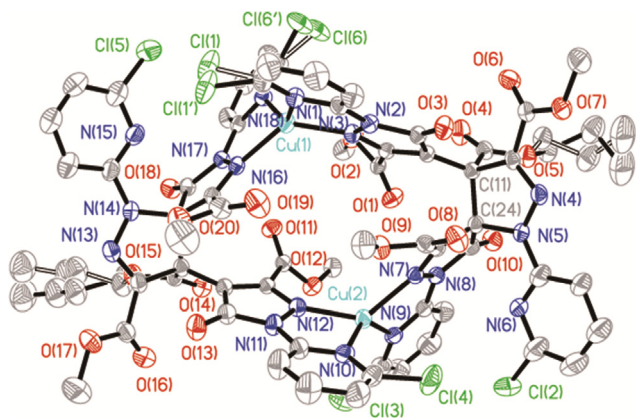


Fig. 5 Molecular structure of **5**. Displacement ellipsoids are drawn at 30% probability level. H atoms are omitted for clarity.

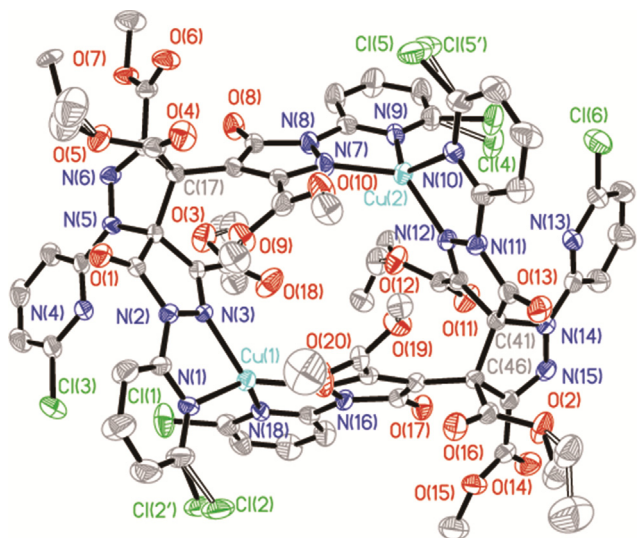


Fig. 6 Molecular structure of **6**. Displacement ellipsoids are drawn at 30% probability level. H atoms are omitted for clarity.

Cu^I ions, and two acetonitrile molecules. In **2**, the Cu1 atom is coordinated by four nitrogen atoms from two different *L*¹ ligands, forming a distorted tetrahedral geometry. The Cu1-N1, Cu1-N3, Cu1-N16, and Cu1-N18 distances are 2.045(4), 1.989(4), 2.011(4), and 2.066(4) Å, respectively (Table S2). Cu2 is also tetra-coordinated by four nitrogen atoms from two different *L*¹ ligands, forming a distorted tetrahedral geometry. The Cu2-N12, Cu2-N7, Cu2-N10, and Cu2-N9 distances are 1.996(4), 1.994(4), 2.038(4), and 2.095(4) Å, respectively. Two pyrazole-pyridyl rings of the *L*¹ ligand link the two Cu atoms to construct a dinuclear complex. Therein, two copper ions and two *L*¹ ligands form a pore with dimensions of approximately 6.146 × 9.275 Å while the Cu1...Cu2 distance is 6.146 Å and the C12...C43 distance is 9.275 Å. It should be noted that the four ester carbonyl groups control the entrance and exit of small molecules to and from the pore. It is interesting to note that the *L*¹ ligand presents as a monovalent anion and exhibits a η¹:η¹:η¹:η¹-μ₂ coordination mode. It should also be pointed out that the *L*¹ ligand is formed *in-situ* reaction and forms two chiral centers (C11(R), C12(R) or C42(R), C43(R)). However, complex **2** is not a chiral molecule and possesses a symmetry centre because the two chiral *L*¹ ligands form mesomers. The dinuclear complex **2** forms a one-dimensional chain through intermolecular Cl...Cl and Cl...O halogen bonds (Cl6...Cl6a, 3.330 Å, Cl3...Cl3b, 3.577 Å, O6...Cl5a, 3.139 Å, symmetry codes: (a) -x, 1-y, -z; (b) -x, 2-y, 1-z, Fig. S3).

Additionally, the atomic valences for two copper ions of **2-6** can be determined by the bond valence model (Brown and Altermatt, 1985; Brese and O'keeffe, 1991; Brown, 2009). According to this model, the sum of all the bond valences around any ion is equal to its ionic charge or valence. Herein, bond valences (*s*) are calculated as $s = \exp[r_0 - r]/B$; $B = 0.37$, $r_0 = 1.61$ for Cu(II)-N pairs from the reference (Brown and Altermatt, 1985; Brese and O'keeffe, 1991). The calculated results are listed in Table S2. Evidently, the calculated values of bond valence sum are in good agreement with the values of expected atomic valence, that is to say, the two copper cations of **2-6** have a valence state of +1 (Table S3).

For **1-6**, the end group is disordered. For example, the three methyl of the ester base groups in **1** is disordered over two sets of sites in a 0.36:0.64 ratio. The methyl (C48, C48', C46, C46') of **2**, ethyl (C16-C17, C16'-C17', C48-C49, C48'-C49', C60, C60'-C61') of **3** and C54-C55, C54'-C55') of **4** and C13-C14-C15, C13'-C14'-C15') of **5**, n-butyl (C46-C47-C48-C49, C46'-C47'-C48'-C49') of **5** in the ester base groups are disordered over two sets in 0.49:0.51, 0.37:0.63, 0.43:0.57, 0.43:0.57, 0.29:0.71, 0.29:0.71 ratio, respectively. In compound **6**, there were methyl ester and ethyl ester in the same position, and their occupations were 0.68 and 0.32, respectively.

2.3. Quantum calculation for **1**

In order to further characterize the energies and conformations of the OH and NH groups in **1**, density functional theory analysis was performed (Fig. S4). The geometric optimization was performed at the b3lyp/cc-pVDZ level of theory, followed by single-point of energy calculations at the MP2/cc-pVTZ level. All the calculations were performed using ORCA 2.9.1 (Neese, 2012) together with the RIJCOSX approximation (Kossmann

and Neese, 2010). According to the results; the conformation of OH for **1** is more stable than that of NH for **1** by approximately 8.4 kcal/mol. Closer study revealed that an O-H...O intramolecular hydrogen bond in OH contributes to the stabilization of the molecule. The short H...O distance (1.653 Å) and the almost linear configuration of the O-H...O moiety confirms the formation of the hydrogen bond. It must be noted that there does not exist O-H...O hydrogen bond in **1** of the crystal structure.

2.4. In vitro anti-tumour activity assays

The cytotoxic activity of **1–4**, Cu(NO₃)₂·3H₂O, cisplatin complexes was examined in HepG2, Capan-2, A549, HeLa, NP69, MGC803 and HUVECs cell lines. Results of MTT assay were presented as IC₅₀ (μM) values for each compound after 48 h of treatment (Table 2).

Compounds **1** and **2** were incubated with the cell lines at concentrations of 4, 8, 16, 32, and 64 μM, and compounds **3** and **4** was incubated with the cell lines at concentrations of 1, 2, 4, 8, 16 μM for 48 h under the same experimental conditions. It was found that compounds **1–4** exhibit different activities towards normal cells and cancer cells (Figs. S5–S8). With the increase in concentration, the inhibitory rate of compounds **1–4** on all selected cell lines increased, except for compound **1** on NP69.

The IC₅₀ values are shown in Table 2 to further illustrate the results. Therefore, compound **2** showed greater selective cytotoxicity towards Hep-G2, Capan-2, HeLa cancer cells after 48 h treatment, in comparison with the standard drug cisplatin (Qin et al., 2018; Qin et al., 2018; Qin et al., 2015; Zhang et al., 2019). The IC₅₀ values of compounds **3** and **4** are lower than that of cisplatin. The results indicate that Compounds **3** and **4** have broad anti-cancer activity. However, The cytotoxic effect of **4** on normal HUVEC cells is significantly reduced and is lower than the cytotoxicity of cisplatin on normal HUVEC cells. These results indicate that compound **2–4** may be a good substitute for platinum-based drugs as a potential antitumor drugs (Psomas and Kessissoglou, 2013; Brown et al., 1980).

2.5. Cell apoptosis assay

Compound **2** induces significantly more apoptosis in HeLa cells compared with **1** (Fig. 7). After incubated with **2** (5 μg/mL, 10 μg/mL, 15 μg/mL) and **1** (20 μg/mL) for 24 h, the HeLa

cancer cells were stained by Annexin V-FITC (FITC is fluorescein isothiocyanate) and PI (propidium iodide) and examined by flow cytometry. As shown in Fig. 3, the percentage of **2** (15 μg/mL) and **1** (20 μg/mL), promoting cell apoptosis were 69.1% and 3.5%, respectively. These results also suggested that **2** (15 μg/mL) was more effective in promoting cell apoptosis than **1** (20 μg/mL). As the concentration of compound **2** increased from 5 μg/mL to 15 μg/mL, the apoptosis rate of HeLa cell lines increased from 7.3% to 69.1%. These results indicate that apoptosis in HeLa cell lines by **2** presents a dose–response relationship.

2.6. Morphology assay

The cell apoptosis in NP69, A549, Capan-2, HeLa, HepG2, and HUVECs cell lines induced by compound **2** was further affirmed by cellular morphology observations (Fig. 8). After the NP69, A549, Capan-2, HeLa, HepG2, and HUVECs cells were incubated with compound **2** at a concentrations gradient of 8–16 μg/mL for 24 h, the changes in cell morphology were observed with an inverted fluorescent microscope (10 ×). As shown in Fig. 4, most of the NP69, A549, Capan-2, HeLa, HepG2, and HUVECs cells in the control group present a normal outline. However, those cell lines exposed to compound **2** shows a clear change in cell morphology. The densities of the tumour cells treated with **2** are lower than those of the control group, indicating that **2** plays a key role in inhibiting cell proliferation. In addition, with an increase in the concentration of **2**, morphological changes in the cells are observed with the cells beginning to become round and some of the cells losing cohesion (some even become suspensions), confirming that **2** induces apoptosis in the tested tumour cells. At the same concentration of **2**, the degree of apoptosis in HeLa cells was greater than that in the other cell lines. However, for the normal NP69 line (Fig. 4a), the shape of the cells in the treatment and control groups are the same, indicating that the cytotoxicity of **2** towards the normal cell NP69 is very low. Thus, these results indicate that **2** can induce apoptosis in Capan-2, HeLa, HePG2, HUVECs, and A549 cells in a dose-dependent manner. The results are consistent with those of the MTT assays above.

2.7. IR spectrum

The IR spectral data of compounds **1–6** are shown in Fig. S16–S21. All the characteristic groups of a series of compounds

Table 2 IC₅₀ values (μM) of cisplatin, Cu(NO₃)₂·3H₂O and **1–4** towards different cell lines ^[a]

Cells	1	2	3	4	Cu(NO ₃) ₂ ·3H ₂ O	cisplatin
HepG2	40.39 ± 1.69	4.50 ± 1.80	1.86 ± 0.11	4.57 ± 0.88	>150	14.06 ± 0.33
Capan-2	38.70 ± 1.04	8.17 ± 0.62	1.07 ± 0.05	6.35 ± 0.76	>150	12.02 ± 0.08
A549	>100	25.73 ± 0.51	2.52 ± 0.68	8.56 ± 0.86	>150	9.48 ± 0.35
HeLa	>100	3.514 ± 1.02	3.84 ± 0.08	5.90 ± 0.09	>150	12.28 ± 1.69
NP69	>100	79.43 ± 39.52	—	—	>150	—
MGC803	—	—	1.15 ± 0.02	3.65 ± 0.18	>150	15.02 ± 1.99
HUVECs	36.31 ± 0.98	6.33 ± 0.34	1.89 ± 0.30	9.00 ± 0.38	>150	6.85 ± 0.35

[a] The IC₅₀ values are the concentrations at which 50% of cells was viable, relative to the control. Data represent the mean ± standard deviation (SD) of three independent experiments performed in triplicate. “—” indicates that the test was not performed.

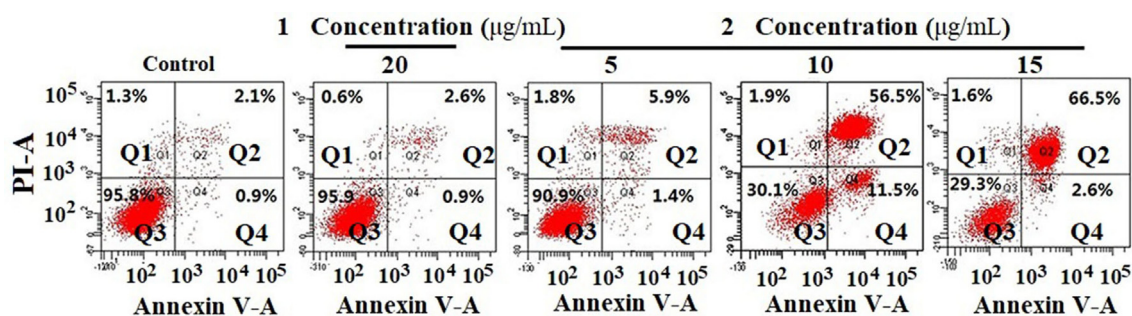


Fig. 7 Induced apoptosis in HeLa by 1 and 2 for 24 h.

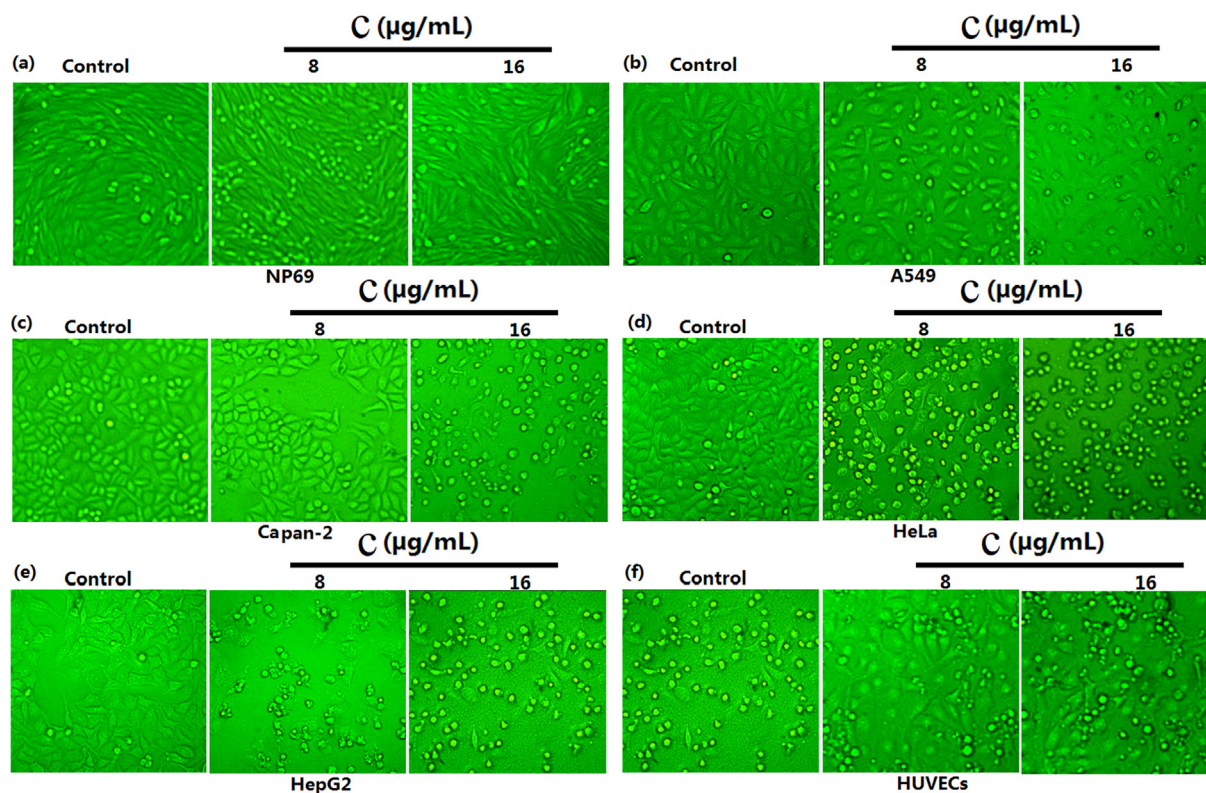


Fig. 8 Morphology observation of six selected cells treated by 8, 16 µg/mL of 2 for 24 h.

exhibited obvious absorption peaks as shown in the IR spectrum. The compounds 1–6 showed a *br* absorption band at 3414–3450 cm^{-1} (O – H), because of the stretching vibration adsorption peak of crystal solution molecules in the air or in the complexes (Liang et al., 1994). Bands at 3103, 3133, 3124, 3115, 3133 cm^{-1} are attributed to the stretching vibration adsorption peak of the group = C-H for compounds 1–4, 6, respectively (Baryshnikov et al., 2013). The bands at 1736–1728 cm^{-1} were attributed to the $\nu(\text{C} = \text{O})$ of the ester group on the compounds 1–6. The bands at 1632–1628 cm^{-1} were attributed to the $\nu(\text{C} = \text{N})$ of the compounds 1–6 while the bands at 1588–1581 cm^{-1} were attributed to the skeleton oscillation of pyridine rings of the compounds 1–6. The bands at 798–786 cm^{-1} were attributed to characteristic absorption peaks of 1,6-disubstituted pyridine in the compounds 1–6 while The bands at 1439–1428 cm^{-1} were attributed to the in-plane bending vibration of $\delta_{\text{as}}(\text{C} = \text{N})$ in the compounds 1–6

(Gusev et al., 2017). The bands at 1235, 1242, 1222, 1228, 1225, 1226 cm^{-1} were attributed to the stretching vibration adsorption peak of the group = C-O- for 1–6, respectively while the bands at 1145, 1123, 1123, 1127, 1128, 1126 cm^{-1} were attributed to the stretching vibration adsorption peak of the group -C-O- for 1–6, respectively.

3. Experimental section

3.1. Materials and instrumentation

All chemicals were commercially available and used as received without further purification. methanol (Xilong Chemical Co., Ltd), ethanol (Xilong Chemical Co., Ltd), acetonitrile (Xilong Chemical Co., Ltd), $\text{Cu}(\text{NO}_3)_2 \cdot 3\text{H}_2\text{O}$ (Xilong Chemical Co., Ltd), n-propanol(Xilong Chemical Co., Ltd), n-butanol

(Xilong Chemical Co., Ltd), **a** (Lab homemade). Elemental analyses (CHN) were performed using an Elemental Vario-EL CHN elemental analyzer. FT-IR spectra were recorded from KBr pellets in the range of 4000–400 cm^{-1} on a Bio-Rad FTS-7 spectrophotometer. The nuclear magnetic resonance spectra of ^1H and ^{13}C were recorded on a Bruker AV500 spectrometer using tetramethylsilane (TMS) as an internal standard and CDCl_3 was used as a solvent. On a Bruker HTC aerosol mass spectrometer records an ESI-MS spectrum. Using the Agilent G8910A CCD diffractometer and SHELXS-18, SHELXL-18 software for X-ray crystal structure was determined for structure resolutions and refinements, respectively. Seven human tumor cell lines, HepG2, Capan-2, A549, HeLa, MGC803, HUVECs and one normal liver cell lines NP69 were all obtained from the Chinese Academy of Sciences Shanghai Cellular Bank. The geometries optimization energy calculations were performed by ORCA 2.9.1 program at MP2/cc-pVTZ level.

3.2. Synthesis

5-acetoxy-1-(6-chloropyridin-2-yl)-1H-pyrazole-3-carboxylic acid methyl ester (**a**) was synthesized according to the procedure reported in literature (Huang et al., 1813).

3.2.1. Synthesis of Htcdodtta (**1**)

A mixture of **a** (0.296 g, 1.0 mmol), methanol (8 mL) and acetonitrile (8 mL) was put into a Teflon-lined autoclave (25 mL) and then heated at 80 °C for 3 d. White crystals of **1** were collected by filtration, washed with methanol and dried in air. Yield: 0.138 g (51.4% based on **a**). *Anal. Calc.* for **1**: $\text{C}_{30}\text{H}_{22}\text{Cl}_3\text{N}_9\text{O}_9$ (756.89), *calc.*: C, 47.61; H, 2.66; N, 16.65%; Found: C, 47.52; H, 2.73; N, 16.72%. ^1H NMR (CDCl_3 , 500 MHz, Fig. S15) δ 1.22 (m, 2H), 3.75 (s, 6H), 3.91 (s, 3H), 7.20 (d, $J = 8.0$ Hz, 1H), 7.28 (s, 1H), 7.69–7.72 (m, 1H), 7.86–7.89 (m, 4H), 7.94 (d, $J = 8.5$ Hz, 1H), 8.00 (d, $J = 8.0$ Hz, 1H) ppm. ^{13}C NMR (CDCl_3 , 500 MHz, Fig. S16) δ 18.4, 52.5, 52.6, 52.6, 95.0, 97.6, 111.1, 111.6, 113.3, 121.8, 121.9, 121.9, 140.3, 141.1, 142.2, 142.3, 145.0, 147.6, 147.7, 149.1, 149.4, 150.3, 152.7, 153.1, 153.3, 156.1, 160.4, 162.3, 162.5, 172.2 ppm. ESI-MS(-MS, Fig. S15): 754.0. IR data for **1** (KBr, cm^{-1}): 3434 w, 3103 w, 1736 m, 1631 w, 1588 s, 1439 s, 1306 m, 1242 m, 1145 m, 1059 w, 896 w, 798 m, 714 w.

3.2.2. $[\text{Cu}_2(\text{L}^1)_2] \cdot (\text{CH}_3\text{CN})$ (**2**)

A mixture of **a** (0.5 mmol, 0.148 g), $\text{Cu}(\text{NO}_3)_2 \cdot 3\text{H}_2\text{O}$ (2 mmol, 0.484 g), methanol (4 mL) and acetonitrile (4 mL) was infused into a Teflon-lined autoclave (25 mL) and then heated at 80 °C for 3 d. The red crystals of **2** were collected by filtered, washed with methanol and drying in air (yield: 0.073 g, *ca.* 50.3%, based on **a**). *Anal. Calc.* for **2**: $\text{C}_{64}\text{H}_{45}\text{Cl}_6\text{Cu}_2\text{N}_{19}\text{O}_{20}$ (1739.97), *calc.*: C, 44.18; H, 2.61; N, 15.29%; Found: C, 44.22; H, 2.69; N, 15.36%. IR data for **2** (KBr, cm^{-1}): 3414 s, 3133 m, 1728 m, 1630 m, 1581 m, 1432 s, 1404 m, 1313 w, 1235 w, 1123 m, 791 w.

3.2.3. $[\text{Cu}_2(\text{L}^2)_{1.63}(\text{L}^3)_{0.37}] \cdot (\text{CH}_3\text{OH})_{0.5}$ (**3**)

Complex **3** was prepared in a similar way to **2**, except that mixed solution (methanol (8 mL) and acetonitrile (8 mL))

was replaced by mixed solution (ethanol (8 mL) and acetonitrile (8 mL)). Red crystals of **3** were obtained (yield: 0.086 g, *ca.* 58.4%, based on **a**). Analysis calculated (%) for **3**, $\text{C}_{66.13}\text{H}_{51.25}\text{Cl}_6\text{Cu}_2\text{N}_{18}\text{O}_{20.5}$: (1765.84), *calc.*: C, 44.98; H, 2.96; N, 14.28%; Found: C, 44.91; H, 3.04; N, 14.033%. IR data for **3** (KBr, cm^{-1}): 3414 s, 1728 m, 1630 m, 1581 s, 1432 s, 1313 w, 1123 s, 798 w.

3.2.4. $[\text{Cu}_2(\text{L}^3)(\text{L}^4)] \cdot (\text{C}_2\text{H}_5\text{OH})_{0.5} \cdot (\text{CH}_3\text{OH})_{0.5}$ (**4**)

Complex **4** was prepared in a similar way to **3**, except that mixed solution ((ethanol (8 mL) and acetonitrile (8 mL)) was replaced by mixed solution (ethanol (4 mL), n-propanol (4 mL) and acetonitrile (8 mL)). Red crystals of **4** were obtained (yield: 0.078 g, *ca.* 52.6%, based on **a**). Analysis calculated (%) for **4**, $\text{C}_{66.5}\text{H}_{53}\text{Cl}_6\text{Cu}_2\text{N}_{18}\text{O}_{21}$ (1780.05), *calc.*: C, 44.87; H, 3.00; N, 14.16%; Found: C, 44.78; H, 3.08; N, 14.23%. IR data for **4** (KBr, cm^{-1}): 3451 s, 1732 s, 1633 m, 1584 s, 1435 s, 1222 m, 1299 w, 1129 m, 789 w, 738 w.

3.2.5. $[\text{Cu}_2(\text{L}^4)(\text{L}^5)] \cdot (\text{H}_2\text{O})$ (**5**)

Complex **5** was prepared in a similar way to **4**, except that mixed solution (ethanol (4 mL), n-propanol (4 mL) and acetonitrile (8 mL)) was replaced by mixed solution (n-propanol (4 mL), n-butanol (4 mL) and acetonitrile (8 mL)). Red crystals of **5** were obtained (yield: 0.088 g, *ca.* 59.09%, based on **a**). Analysis calculated (%) for **5**, $\text{C}_{67}\text{H}_{54}\text{Cl}_6\text{Cu}_2\text{N}_{18}\text{O}_{21}$ (1787.06), *calc.*: C, 45.03; H, 3.05; N, 14.11%; Found: C, 44.94; H, 3.13; N, 14.19%. IR data for **5** (KBr, cm^{-1}): 3458 s, 1732 s, 1633 m, 1584 s, 1435 s, 1314w, 1222 m, 1129 m, 789 w, 732 w.

3.2.6. $[\text{Cu}_2(\text{L}^1)_{1.18}(\text{L}^2)_{0.82}]$ (**6**)

Complex **6** was prepared in a similar way to **3**, but the reaction time is reduced by half. Red crystals of **6** were obtained (yield: 0.078 g, *ca.* 52.6%, based on **a**). Analysis calculated (%) for **6**, $\text{C}_{63.64}\text{H}_{45.28}\text{Cl}_6\text{Cu}_2\text{N}_{18}\text{O}_{20}$ (1721.92), *calc.*: C, 44.39; H, 2.65; N, 14.64%; Found: C, 44.32; H, 2.74; N, 14.70%. IR data for **6** (KBr, cm^{-1}): IR data for **6** (KBr, cm^{-1}): 3414 s, 1729 m, 1628 m, 1580 s, 1432 s, 1311 w, 1122 s, 799 w.

3.3. In vitro cytotoxicity assay

Cell lines: HepG2, Capan-2, A549, HeLa, NP69, HUVECs, MGC803 were from the Chinese Academy of Sciences Shanghai Cellular Bank. Cell lines were germinated in RPMI-1640 medium supplemented with 10% (v/v) fetal bovine serum, 100 U/mL penicillin, 2 mM glutamine, and 100

U/mL streptomycin at 37 °C, in a highly humidifying the atmosphere of 95% air and 5% CO_2 . **1**–**4**, $\text{Cu}(\text{NO}_3)_2 \cdot 3\text{H}_2\text{O}$ and cisplatin are cytotoxic to HepG2, Capan-2, A549, HeLa, NP69, HUVECs, MGC803 cell lines examined by the micro-culture tetrazolium (MTT) assay (Alley et al., 1988). The experiment was carried out by the reporting procedure (Chen et al., 2013). The inhibition rate of cell growth was calculated with the data from three repeated trials by $(\text{OD}_{\text{control}} - \text{OD}_{\text{test}}) / \text{OD}_{\text{control}} \times 100\%$. Compounds **1**, **2** were incubated with cell lines for 48 h with gradient of concentration in 4 μM , 8 μM , 16 μM , 32 μM , 64 μM , while Compounds **3**, **4** did with cell lines for 48 h with gradient of concentration in 1 μM , 2 μM , 4 μM , 8 μM , 16 μM .

Table 3 Crystallographic and experimental data for the complexes 1–6.

Compounds	1	2	3	4	5	6
Formula	C ₃₀ H ₂₅ Cl ₃ N ₉ O ₉	C ₆₂ H ₄₂ Cl ₆ Cu ₂ N ₁₈ O ₂₀ .CH ₃ CN	C _{56.63} H _{49.25} Cu ₂ N ₁₈ O ₂₀ .Cl ₆ .0.5CH ₃ OH	C ₆₅ H ₄₈ Cl ₆ Cu ₂ N ₁₈ O ₂₀ .0.5C ₂ H ₅ OH.0.5CH ₃ OH	C ₆₇ H ₅₂ Cu ₂ N ₁₈ O ₂₀ Cl ₆ .H ₂ O	C _{63.64} H _{45.28} Cl ₆ Cu ₂ N ₁₈ O ₂₀
Form. weight	756.90	1739.97	1765.83	1780.07	1787.08	1721.91
Crystal system	triclinic	triclinic	Monoclinic	Triclinic	Triclinic	Monoclinic
Space group	$P\bar{1}$	$P\bar{1}$	$P2_1/c$	$P\bar{1}$	$P\bar{1}$	$P2_1/c$
<i>a</i> /Å	11.254(1)	13.470(1)	14.346(1)	14.894(2)	14.698(1)	14.250(1)
<i>b</i> /Å	12.279(1)	15.595(1)	22.133(1)	17.608(2)	17.766(1)	22.207(1)
<i>c</i> /Å	15.763(2)	18.386(1)	23.527(1)	19.021(1)	19.000(1)	23.365(1)
α /°	84.46(1)	84.543(4)	90.00	113.84(1)	113.556(3)	90.00
β /°	71.68(1)	85.261(4)	97.326(3)	94.06(1)	93.761(3)	97.064(4)
γ /°	65.53(1)	75.794(4)	90.00	113.71(1)	114.025(3)	90.00
<i>V</i> /Å ³	1880.6(4)	3720.1(3)	7409.5(5)	4012.3(8)	3996.6(3)	7337.9(5)
<i>Z</i>	2	2	4	2	2	4
<i>D</i> _{calcd.} /gcm ⁻³	1.337	1.553	1.583	1.473	1.485	1.559
μ /mm ⁻¹	0.304	0.872	0.877	0.811	0.814	0.883
<i>R</i> _{int}	0.0218	0.0453	0.0790	0.0594	0.0432	0.0477
Goof	0.993	1.004	1.033	1.014	0.984	0.995
Completeness	99.6%	99.8%	98.9%	99.5%	99.7%	99.7%
<i>F</i> (000)	772	1764	1796.05	1812	1820	3492.4
θ range/°	2.89 to 25.01	2.88 to 25.10	2.90 to 25.10	3.01 to 25.01	2.84 to 25.01	2.88 to 25.01
Ref.coll./unique	15462/6623	28310/13198	35,646/13,075	29,875/14,091	32,089/14,059	34765/12893
Obs. ref. $[I > 2\sigma(I)]$	4861	8090	6307	7763	9834	7597
No. of parameters	475	1045	1053	1007	1055	1043
Final <i>R</i> ₁ $[I > 2\sigma]$ ^[a]	0.0525	0.0693	0.1149	0.0800	0.0605	0.0680
<i>wR</i> ₂ ^[b]	0.1482	0.2034	0.2335	0.2368	0.1826	0.2259
Residues/eÅ ⁻³	0.425 and -0.389	0.964 and -0.441	0.629 and -0.582	0.870 and -1.079	0.997 and -0.808	0.838 and -0.614

[a] $R_1 = \frac{\sum ||F_o| - |F_c||}{\sum |F_o|}$. [b] $wR_2 = \frac{[\sum w(|F_o|^2 - |F_c|^2)|^2]}{\sum w(|F_o|^2)}^{1/2}$.

3.4. Cell apoptosis assay

According to the manufacturer's instructions, apoptosis was detected with an Annexin V/PI kit purchased from BD Pharmingen (BD Bioscience). HeLa cells were implanted in 6-hole plates, and were allowed to grow into 75–85% confluence. HeLa cell was treated with **2** and **1** (10 and 15 $\mu\text{g}/\text{mL}$) for 24 h. To detect early and late apoptosis, floating and adherent cells were harvested and washed twice with $1 \times \text{PBS}$, and were centrifuged at 1000 r.min⁻¹ for 5 min removed the medium, and were resuspension of binding buffer 200 μL at a density of 106 cells per mL. Subsequently, annexin V-FITC (5 μL) were added to the binding buffer for stain cells. At 37 °C in the dark, Cells lines were incubated for 10 min, and were centrifuged at 1000 r.min⁻¹ for 5 min for removing the binding buffer, and were resuspension of binding buffer 200 μL again. PI (propidium iodide, 5 μL) were added to the binding buffer for stain cells, and cells lines were analyzed by a FACS Calibur (BD Bioscience).

3.5. Morphological characterization of cell apoptosis

logarithmic phase cells were seeded into 96-hole plates with cell density of $8 \times 10^3/\text{hole}$ in a moist incubator (37 °C and 5% CO_2 , 95% air). Cell morphology observation further confirmed that the cell apoptosis of NP69, A549, Capan-2, HeLa, HePG2, HUVECs were induced by **2**. At gradient concentrations of 8, 16 $\mu\text{g}/\text{mL}$, the NP69, A549, Capan-2, HeLa, HePG2, HUVECs cells were treated with **2** for 24 h, then the cells lines were further treated for 48 h at incubator. The morphology of the cells was imaged using an inverted microscope ($10 \times$).

3.6. X-ray crystallography

Single-crystal X-ray diffraction data for **1–6** were collected by SuperNova, Single source at offset, Eos with graphite monochromated Mo-K α radiation ($\lambda = 0.71073 \text{ \AA}$) at 293 K using the ω scan mode in the ranges $2.89^\circ \leq \theta \leq 25.01^\circ$ (**1**), $2.88^\circ \leq \theta \leq 25.10^\circ$ (**2**), $2.90^\circ \leq \theta \leq 25.10^\circ$ (**3**), $3.01^\circ \leq \theta \leq 25.01^\circ$ (**4**), $2.84^\circ \leq \theta \leq 25.01^\circ$ (**5**), $2.88^\circ \leq \theta \leq 25.01^\circ$ (**6**), respectively. The raw frame data were integrated with the Cry-sAlisPro program. The structures were solved directly by using SHELXS-97 and the structures were refined by full-matrix least-squares on F^2 using SHELXL-2018 (Sheldrick, 2015) within the OLEX-2 GUI (Dolomanov et al., 2009). An empirical absorption correction was performed on the program spherical harmonics, implemented in SCALE3 ABSPACK scaling algorithm. Compound **1** had a disordered solvent water molecule; and the disordered water molecule was processed by the squeeze software. All of the non-hydrogen atoms were refined anisotropically. All of the hydrogen atoms were arranged in the geometry and they were refined for riding. For The selected bond distances and angles of the compounds **1–6**, are provided in Tables S1, S2. The crystallographic data of the compounds **1–6** are reported in Table 3.

4. Conclusions

Six novel compounds, Htcdodtta (**1**), $[\text{Cu}_2(\text{L}^1)_2] \cdot (\text{CH}_3\text{CN})$ (**2**), $[\text{Cu}_2(\text{L}^2)_{1.63}(\text{L}^3)_{0.37}] \cdot (\text{CH}_3\text{OH})_{0.5}$ (**3**), $[\text{Cu}_2(\text{L}^3)(\text{L}^4)] \cdot (\text{C}_2\text{H}_5\text{OH})_{0.5} \cdot (\text{CH}_3\text{OH})_{0.5}$ (**4**), $[\text{Cu}_2(\text{L}^4)(\text{L}^5)] \cdot (\text{H}_2\text{O})$ (**5**) and $[\text{Cu}_2(\text{L}^1)_{1.18}(\text{L}^2)_{0.82}]$ (**6**) have been synthesized. Compound **2** exhibited enhanced cytotoxicities against Capan-2, HeLa and HepG2 cell lines and Compounds **3** and **4** exhibit antitumor activity against HeLa, Capan-2, HepG2, MGC803, and A549 cell lines while the cytotoxicity of compound **4** to normal cells is lower than that of compound **3** and cisplatin. The IC_{50} values of compounds **2–4** against the HepG2, Capan-2, HeLa cell lines were in the range 1.07–8.56 μM , with compound **3** showing the highest potency against the Capan-2 cell line, while The IC_{50} values of **1** are $> 36.31 \pm 0.98 \mu\text{M}$ for all experimental cells. The results indicate that adjusting the water solubility of the compounds can adjust the anticancer activity of the compounds **2–4**. In addition, compound **2** effectively induces cell apoptosis in HeLa cell in a dose-dependent manner and changes morphological of the Capan-2, HeLa, HePG2, HUVECs and A549 cell lines.

Authors' contributions

Yanhui Qiao synthesized and characterized compounds **1–3**; Yating Chen synthesized and characterized compounds **4,5**; Qiuping Huang interpreted the results. Yujie Zhang synthesized and characterized compound **6**. Guangzhao Li wrote and revised the manuscript; Shuhua Zhang designed the study, and revised the manuscript. All authors commented on the manuscript. All authors read and approved the final manuscript.

Declaration of Competing Interest

The authors declare that they have no competing interests.

Acknowledgements

This work was supported by the Nature Science Foundation of China (No. 21861014), Program of the Collaborative Innovation Center for Exploration of Hidden Nonferrous Metal Deposits and Development of New Materials in Guangxi (No. GXYSXTZX2017-II-3), Talent Introduction Project of Guangdong University of Petrochemical Technology (No. 2020rc033) and Middle-aged and Young Teachers' Basic Ability Promotion Project of Guangxi (No. 2019KY0769).

Appendix A. Supplementary data

Supplementary data to this article can be found online at <https://doi.org/10.1016/j.arabjc.2021.103237>.

References

Ali, A.R., El-Bendary, E.R., Ghaly, M.A., Shehata, I.A., 2014. Eur. J. Med. Chem. 75, 492.

- Allen, F.H., Davies, J.E., Galloy, J.J., Johnson, O., Kennard, O., Macrae, C.F., Mitchell, E.M., Mitchell, G.F., Smith, J.M., Watson, D.G., 1991. *J. Chem. Inf. Comput. Sci.* 31, 187.
- Alley, M.C., Scudiero, D.A., Monks, A., Hursey, M.L., Czerwinski, M.J., Fine, D.L., Abbott, B.J., Mayo, J.G., Shoemaker, R.H., Boyd, M.R., 1988. *Cancer. Res.* 48, 589.
- Ambika, S., Arunachalam, S., Arun, R., Premkumar, K., 2013. *RSC Adv.* 3, 16456.
- Anzai, K., Furuse, M., Yoshida, A., Matsuyama, A., Moritake, T., Tsuboi, K., Ikota, N., 2004. *J. Radiat. Res.* 45, 319.
- Badawey, E.-S.A.M., El-Ashmawey, I.M., 1998. *Eur. J. Med. Chem.* 33, 349.
- Bailey, D.M., Hansen, P.E., Hlavac, A.G., Baizman, E.R., Pearl, J., Defelice, A.F., Feigenson, M.E., 1985. *J. Med. Chem.* 28, 256.
- Baryshnikov, G.V., Minaev, B.F., Korop, A.A., Gusev, A.N., 2013. *Russ. J. Inorg. Chem.* 58 (8), 928–934.
- Brese, N.E., O'keeffe, M., 1991. *Acta Cryst.* B47, 192.
- Brown, I.D., 2009. *Chem. Rev.* 109, 6858.
- Brown, I.D., Altermatt, D., 1985. *Acta Cryst.* B41, 244.
- Brown, D.H., Smith, W.E., Teape, J.W., Lewis, A.J., 1980. *J. Med. Chem.* 23, 729.
- Budzisz, E., Miernicka, M., Lorenz, I.-P., Mayer, P., Krajewska, U., Rozalski, M., 2009. *Polyhedron* 28, 637.
- Cao, Q., Zhou, D.-J., Pan, Z.-Y., Yang, G.-G., Zhang, H., Ji, L.-N., Mao, Z.-W., 2020. *Angew. Chem. Int. Edit.* 59, 18556.
- F. A. Carey, R.J. Sundberg, *Advanced Organic Chemistry, Part A, Structure and Mechanisms*, 5th ed; Springer Science + Business Media: Boston, MA, USA, 2007.
- Chen, Z.F., Qiong, Y.Q., Song, X.Y., Liu, Y.C., Peng, Y., Liang, H., 2013. *Eur. J. Med. Chem.* 59, 19–202.
- Ciolkowski, M., Paneth, P., Lorenz, I.P., Mayer, P., Rozalski, M., Krajewska, U., Budzisz, E., *EnzymInhib. J.*, 2009. *Med. Chem.* 24, 1257.
- Darrenm, G., James, P.P., Celine, J.M., 2010. *Med Chem. Anti-Cancer. Agents.* 10, 354.
- Das, N., Verma, A., Shrivastava, P.K., Shrivastava, S.K., 2008. *Indian. J. Chem. B.* 47, 1555.
- Dolomanov, O.V., Bourhis, L.J., Gildea, R.J., Howard, J.A.K., Puschmann, H., 2009. *J. Appl. Cryst.* 42, 339.
- Fernández-Bachiller, M.I., Pérez, C., González-Muñoz, G.C., Conde, S., López, M.G., Villarroya, M., García, A.G., Rodríguez-Franco, M.I., 2010. *J. Med. Chem.* 53, 4927.
- Fustero, S., Sanchez-Rosello, M., Barrio, P., Simon-Fuentes, A., 2011. *Coord. Chem. Rev.* 111, 6984.
- González-Álvarez, M., Pascual-Álvarez, A., Agudo, L.C., Castiñeiras, A., Liu-González, M., Borrás, J., Alzuet-Piña, G., 2013. *Dalton. Trans.* 42, 10244.
- Gürsoy, A., Demirayak, S., Capan, G., Erol, K., Vural, K., 2000. *Eur. J. Med. Chem.* 35, 359.
- Gusev, A.N., Shul'gin, V.F., Minaev, B.F., Baryshnikov, G.V., Minaeva, V.A., Baryshnikova, A.T., Kiskin, M.A., Eremenko, I. L., 2017. *Russ. J. Inorg. Chem.* 62 (4), 423–430.
- Huang, Q.P., Zhang, S.N., Zhang, S.H., Wang, K., Xiao, Y., 1813. *Molecules* 2017, 22.
- Jiang, J.B., Hesson, D.P., Dusak, B.A., Dexter, D.L., Kang, G.J., Hamel, E., 1990. *J. Med. Chem.* 33, 1721.
- Kalinowska-Lis, U., Szewczyk, E.M., Chęcińska, L., Wojciechowski, J.M., Wolf, W.M., Ochocki, J., 2014. *Chem. Med. Chem.* 9, 169.
- Katsarou, M.E., Efthimiadou, E.K., Psomas, G., Karaliota, A., Vourloumis, D., 2008. *J. Med. Chem.* 51, 470.
- Kossmann, S., Neese, F., 2010. *J. Chem. Theory. Comput.* 6, 2325.
- Liang, H., Zhou, Y.Q., Shen, P.W., 1994. *Chin. Sci. Bull.* 39, 1452.
- Liu, W.K., Gust, R., 2013. *Chem. Soc. Rev.* 42, 755.
- Miernicka, M., Szulawska, A., Czyz, M., Lorenz, I.-P., Mayer, P., Karwowski, B., Budzisz, E., 2008. *J. Inorg. Biochem.* 102, 157.
- Mohareb, R.M., El-Sayed, N.N.E., Abdelaziz, M.A., 2012. *Molecules.* 17, 8449.
- Neese, F., 2012. *WIREs. Comput. Mol. Sci.* 2, 73.
- Ng, N.S., Leverett, P., Hibbs, D.E., Yang, Q.F., Bulanadi, J.C., Wu, M.J., Aldrich-Wright, J.R., 2013. *Dalton. Trans.* 42, 3196.
- Palkar, M.B., Patil, A., Hampannavar, G.A., Shaikh, M.S., Patel, H. M., Kanhed, A.M., Yadav, M.R., Karpoomath, R.V., 1969. *Med. Chem. Res.* 2017, 26.
- Pan, Z.-Y., Tan, C.-P., Rao, L.-S., Zhang, H., Zheng, Y., Hao, L., Ji, L.-N., Mao, Z.-W., 2020. *Angew. Chem. Int. Ed.* 59, 18755.
- Pelosi, G., Bisceglie, F., Bignami, F., Ronzi, P., Schiavone, P., Re, M. C., Casoli, C., Pilotti, E., 2010. *J. Med. Chem.* 53, 8765.
- Psomas, G., Kessissoglou, D.P., 2013. *Dalton. Trans.* 42, 6252.
- Qin, Q.-P., Chen, Z.-F., Qin, J.-L., He, X.-J., Li, Y.-L., Liu, Y.-C., Huang, K.-B., Liang, H., 2015. *Eur. J. Med. Chem.* 92, 302.
- Qin, X.Y., Yang, L.C., Le, F.L., Yu, Q.Q., Sun, D.D., Liu, Y.N., Liu, J., 2013. *Dalton. Trans.* 42, 14681.
- Qin, X.Y., Wang, Y.N., Yang, X.P., Liang, J.J., Liu, J.L., Luo, Z.H., 2017. *Dalton. Trans.* 46, 16446.
- Qin, Q.-P., Wang, S.-L., Tan, M.-X., Wang, Z.-F., Huang, X.-L., Wei, Q.-M., Shi, B.-B., Zou, B.Q., Liang, H., 2018. *Metallomics* 10, 1160.
- Qin, Q.-P., Wang, S.-L., Tan, M.-X., Wang, Z.-F., Luo, D.-M., Zou, B.-Q., Liu, Y.-C., Yao, P.-F., Liang, H., 2018. *Eur. J. Med. Chem.* 158, 106.
- Qin, X.Y., Wang, Y.N., Liu, H.F., Luo, Z.H., Zhang, P.L., Huang, L. F., Liu, M.R., 2020. *Metallomics* 12, 92.
- Sánchez-Delgado, R.A., Navarro, M., Lazardi, K., Atencio, R., Capparelli, M., Vargas, F., Urbina, J.A., Bouillez, A., Noels, A. F., Masi, D., 1998. *Inorg. Chim. Acta* 275–276, 528.
- Sheldrick, G.M., 2015. *Acta Cryst.* C71, 3.
- Tardito, S., Bassanetti, I., Bignardi, C., Elviri, L., Tegoni, M., Mucchio, C., Bussolati, O., Franchi-Gazzola, R., Marchio, L., 2011. *J. Am. Chem. Soc.* 133, 6235.
- Wang, Y., Zhi, Y., Jin, Q., Lu, S., Lin, G., Yuan, H., Yang, T., Wang, Z., Yao, C., Ling, J., Guo, H., Li, T., Jin, J., Li, B., Zhang, L., Chen, Y., Lu, T., 2018. *J. Med. Chem.* 61 (4), 1499.
- Xiao, Y., Huang, P., Liu, Y.Q., 2015. *Mol. Cryst Liq. Cryst.* 607, 242.
- Xiao, Y., Liu, Y.Q., Li, G., Huang, P., 2015. *Supramol. Chem.* 27 (3), 161.
- Yang, P., Zhang, D.-D., Wang, Z.-Z., Liu, H.-Z., Shi, Q.-S., Xie, X.-B., 2019. *Dalton Trans.* 48, 17925.
- Zhang, P.-L., Hou, X.-X., Liu, M.-R., Huang, F.-P., Qin, X.-Y., 2020. *Dalton Trans.* 49, 6043.
- Zhang, H.Y., Wang, W., Chen, H., Zhang, S.H., Li, Y., 2016. *Inorg. Chim. Acta.* 453, 507.
- Zhang, S.M., Zhang, H.Y., Qin, Q.P., Fei, J.W., Zhang, S.H., 2019. *J. Inorg. Biochem.* 193, 52.
- Zhao, X.F., Ouyang, Y., Liu, Y.Z., Su, Q.J., Tian, H., 2014. *New. J. Chem.* 38, 955.